PROCEEDINGS OF THE EIGHTH WORLD CONFERENCE
ON EARTHQUAKE ENGINEERING, VOL.2, 1984

PREDICTION OF STRONG GROUND MOTIONS USING OBSERVED SEISMOGRAMS FROM SMALL EVENTS

K. Irikura(I)

SUMMARY

A synthesis method is developed for estimating deterministically strong ground motions during the mainshock, using the records of small events such as foreshocks and aftershocks which occurred within the area of the mainshock fault. This synthesis formulation is based on the kinematic source model of Haskell type and the similarity law of earthquakes. The parameters for this synthesis are given to be consistent with the scaling relations between the moments and the fault parameters such as fault length, width and dislocation rise time. We compare the mainshock velocity and acceleration motions synthesized by this method with the observed motions for 1980 Izu-Hanto-Toho-Oki Earthquake (M=6.7).

INTRODUCTION

The prediction of strong ground motions during large earthquakes is an important subject of engineering interest. The purpose of this study is to develope a reliable and practical synthesis method of strong ground motions, based on careful considerations of the physical properties of earthquake faults in real media.

Hartzell (1978)(1) proposed an attractive approach to synthesize strong motions from a mainshock by using observed seismograms from aftershocks as Green functions. It is an advantageous method because the Green functions include complex effects due to the dynamic rupture processes on the fault as well as due to the heterogeneous earth structures arround the sources and the observation sites, which are extremely cumbersome to evaluate. However, the method initially attempted by him has some problems which need to be improved. For example, in his method the discrepancy between the dislocation rise time of the mainshock and that of the aftershocks is not taken into account and the number of summation of aftershock records is not specified.

We formulated a semi-impirical synthesis method for estimating the mainshock motions using records of small events such as foreshocks and aftershocks, based on the kinematic source model by Haskell and the similarity law of earthquakes. The parameters for synthesis are determined to be consistent with the scaling relations between seismic moments and fault parameters such as fault length, width and dislocation rise time.

SYNTHESIS METHOD

The strong ground motions during large earthquakes are synthesized

(I) Associate professor, Disaster Prevention Research Institute of Kyoto University, Japan

by the method presented by Irikura (1983)[2]. We outline here the synthesis method.

Kanamori and Anderson (1975)[3] derived the following conditions regarding the similarity of earthquakes:

$$L/W = \text{const} \quad (1)$$
$$D/W = \text{const} \quad (2)$$
$$L/(Vr \cdot \tau) = \text{const} \quad (3)$$

where L and W are the fault length and width, D, the final offset of the dislocation, τ, the rise time, and Vr, the rupture velocity.

Now, we consider two events, with different sizes, which occurred within the same source region, e.g. one is mainshock and the other, foreshock or aftershock. Then the similarity relations between those source parameters are deduced from (1) to (3):

$$L/L_e = W/W_e = D/D_e = \tau / \tau_e = (Mo/Mo_e)^{1/3}, \quad (4)$$

where the parameters without subscript e are for mainshock and those with subscript e, for small events. This relation between the slip D and the rise time τ corresponds to the assumption that the slip velocities are constant for most earthquakes with different sizes. Thus, the dislocation function of the mainshock, ΔU, can be related to that of the small event, ΔU_e:

$$\Delta U(t) = \sum_{k=1}^{N} \Delta U_e[\, t-(k-1)\tau_e] \quad (5)$$

where τ_e is the rise time of the small event. Based on these similarity conditions, the synthesis procedure is introduced as follows. Primarily, the ratio of the mainshock moment to the small event, Mo/Mo_e is determined. When $(Mo/Mo_e)^{1/3}$ is approximated by an integer N, the mainshock fault plane Σ (=L x W) is divided into N x N elements. Then, the area of an element, $\Delta\Sigma$, is taken as the fault size of the small event, Σ_e (= L_e x W_e). The mainshock is considered to be generated by the subsequent occurrences of N small events in an element with a specific time delay to satisfy the above relation (5) and by the subsequent ruptures of N^2 elements as if the ruptures propagate at a certain rupture velocity over the mainshock fault plane, as shown in Fig. 1. That is, the ground motions G(x,t) from the mainshock are given by the time-lagged summation $G_{e_{lm}}$ from small events over the fault plane:

$$G(x,t) = \sum_{k=1}^{N} \sum_{l=1}^{N} \sum_{m=1}^{N} G_{e_{lm}}(\, x, t-t_{d_{klm}}) \quad (6)$$

where $t_{d_{klm}}$ is given as

$$t_{d_{klm}} = r_{lm}/Vc + \sqrt{\xi_l^2 + \eta_m^2}/Vr + (k-1)\cdot\tau_{e_{lm}},$$

r_{lm} is the distance between the element located at (ξ_l, η_m) and the observation site, Vc is the seismic wave velocity (either P or S) and Vr is the rupture velocity.

When synthesizing the mainshock motions employing (6), we need to use all the records from all elements. The practical synthesis method

is revised to use only several small-event records after slight modification.

SYNTHESIS OF THE MAINSHOCK VELOCITY MOTIONS FOR 1980 IZU-HANTO-TOHO-OKI EARTHQUAKE (M=6.7)

1980 Izu-Hanto-Toho-Oki earthquake occurred on June 29, 1980, off the east coast of the Izu Peninsula in Japan. We observed the mainshock as well as several foreshocks and aftershocks at the three sites located at 20-100 km from the epicenters using velocity-type strong-motion-seismographs designed by Muramatu (1977)[4]. The maximum velocity of 8 kine was recorded at the JIZ station on hard rock, about 20 km away from the epicenter. The locations of the observed stations, JIZ, SMC and OMM are shown by (+) mark in Fig. 2. The observation system was designed to record exactly ground velocity motions with the dynamic range from 100 to 0.01 kines over the period range from 0.05 to 50 second.

The synthesis procedure is illustated for the mainshock motions at JIZ as follows.

We use the observed seismograms from two aftershocks, A1 (M=4.9) and A3 (M=4.6). Aftershocks A1 and A3 occurred at the south part and the north part within the mainshock source area, respectively, as shown in Fig. 2. The mainshock focal mechanism determined by Imoto et al (1981) shows strike slip type with strike=N15°W and dip=75°. The both focal mechanisms of aftershocks A1 and A3 are almost the same as that of the mainshock. The fault dimension of the mainshock are estimated to be L=15 km and W=7.5 km from the aftershocks' distribution.

The observed seismograms and the Fourier spectra of the mainshock and the aftershocks at JIZ are shown in Fig. 3 and Fig. 4. The moment ratios, Mo/Mo_e, between the mainshock and the aftershocks are estimated from the spectral ratios between their seismograms, as shown in Fig. 5. Since the seismic moments are proportional to the spectral densities at the frequencies lower than the corner frequencies, the moment ratio Mo/Mo_e is given from the flat level of the spectral ratio in the low frequency range. Then we estimate the moment ratio of the mainshock to aftershock A1 to be about 200 and that of the mainshock to aftershock A3 to be about 350. The scaling parameter N ($\simeq \sqrt[3]{Mo/Mo_e}$) corresponding to the fault length ratio between the two events is given to be 6 for the mainshock versus aftershock A1 and to be 7 for the mainshock versus aftershock A3. The mainshock fault plane is divided into N x N elements and the mainshock hypocenter determined assuming a point source is regarded as the starting point of rupture, as shown in Fig. 6. The rise time of the mainshock is estimated to be 1 sec from the significant trough frequency of the spectra. The rise times of the aftershocks are taken as τ/N from the similarity conditions.

Employing the above parameters and following (6), we make deterministically a synthesis for the mainshock motions using the aftershock records. An example of the synthesized velocity motions is shown in

Fig. 7 together with the observed seismogram of the mainshock for JIZ station. The synthesized motions agree well with the observed ones in the frequency range lower than 1 Hz. The spectral amplitudes of the synthesized motions at the frequencies higher than 1 Hz become significantly smaller than those of the observed ones. The underestimates for the higher frequency motions are caused by the faulting model which is assumed to be a coherent rupture propagation and a constant dislocation given by a linear ramp function over a rectangular fault plane. The source time function based on this model has w^{-3} decay at the frequencies higher than $1/\tau$. To get the high frequency motions consistent with the observed seismograms, the model need to be improved to have w^{-2} decay.

IMPROVEMENT FOR HIGHER FREQUENCY MOTIONS

Ground motions with frequencies higher than 1 Hz play an important role in acceleration motions. We improve the formulation (6) to be applicable to the higher frequency motions. The present revise is based on an idea that the slips on the fault plane during the mainshock are able to be approximately replaced to the folded distributions of the slips during small events along the mainshock fault plane, as shown in Fig. 8. Then, the relation between the mainshock dislocation and the small event one is rewrited as follows

$$U(\xi, \eta, t) = \sum_{k=1}^{N} U_e(\xi - (k-1)\Delta X, \eta, t) \qquad (7)$$

If we use the records from the small event having the length $Le = N\Delta x = Vr\tau$, (6) is rewritten,

$$G(x,t) = \sum_{1'=1}^{N\times N}\sum_{m=1}^{N} G_{e1m}(x, t-t'_{d1'm}) \qquad (8)$$

where $t'_{d1'm} = r_{1'm}/Vc + \sqrt{\xi_{1'}^2 + \eta_m^2}/Vr$ ($\eta_m = (m-1)W_e$, $m = 1,2,---, N$, and $\xi_{1'} = (1'-1)\, L_e/N$, $1' = 1,2,---, N\times N$). The acceleration motions synthesized by (8) have w^{-2} decay if each G_{e1m} has an flat spectrum at high frequencies.

When applying (8) to the synthesis, a smoothing operation need to be made to reduce the ghost oscillatory motions due to the apparent periodicity of $\Delta x/Vr$ (see Ref. 2). In Fig. 9, the waveform and spectrum of the acceleration motions synthesized by the revised method are compared with those of the observed for the case of the same earthquake shown in Fig. 7. The envelope of the synthesized waveform agrees well with that of the observed one, although the two waveforms do not always correspond to each other in individual phases. The spectral amplitudes of the synthesized also agree well with those of the observed one at the frequencies up to 5 Hz.

CONCLUSION

The synthesis method in this paper is based on the representation, including the source effects, relating to the dislocation at every point on the fault plane and to the rupture propagation over the fault plane, and the path effects, relating to the wave propagation from the source

to the site. If there is a certain similarity relation between large earthquakes and small ones within the same source area, this synthesis formulation expresses an accurate approximation for the wave field from the source to the site as far as it can. For the case of 1980 Izu-Hanto-Toho-Oki earthquake, the synthesized velocity motions agree well in the frequency range less than 1 Hz with the observed ones at JIZ station, 20km away from the epicenter.

To be applicable to higher frequency motions, the method is revised by rewriting the relation in time domain between the mainshock dislocation and the small event one to the relation in time-space domain. If we use the records from the small events having the faulth length $Le = Vr\,\tau$, the revised method is effective for higher frequency motions. The synthesized acceleration motions agree well with the observed ones in the frequency range up to 5 Hz.

The author thanks Dr. Kinoshita for providing the digital data obtained at the Nakaizu station (JIZ) of National Research Center for Disaster Prevention, the Science and Technology Agency in Japan.

REFERENCES

1) Hartzell, S. (1978). Earthquake aftershocks as Green's function, Geophys. Res. Letters, 5, 1-4.
2) Irikura, K. (1983). Semi-empirical estimaiton of strong ground motions during large earthquakes, Bull. Disast. Prev. Res. Inst., Kyoto Univ., 33, 63-103.
3) Kanamori, H. and D. L. Anderson (1975). Theoretical basis of some empirical relations in seismology, Bull. Seism. Soc. Am., 65, 1073-1095.
4) Muramatu, I. (1977). A velocity type strong motion seismograph with wide frequency range, J. Seism. Soc. Japan (JISHIN), 30, 317-338 (in Japanese).
5) Imoto, M., I. Karakama, R. S. Matsuura, F. Yamazaki, A. Yoshida and K. Ishibashi (1981). Focal Mechanisms of the 1980 earthquake swarm off the east coast of the Izu Peninsula, Japan, J. Seism. Soc. Japan (JISHIN), 34, 481-493 (in Japanese).

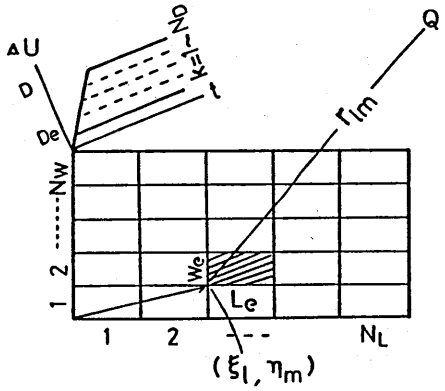

Fig. 1. Mainshock fault plane divided into $N_L \times N_W$ elements. $N_L=N_W=N_D \approx (Mo/Mo_e)^{1/3}$.

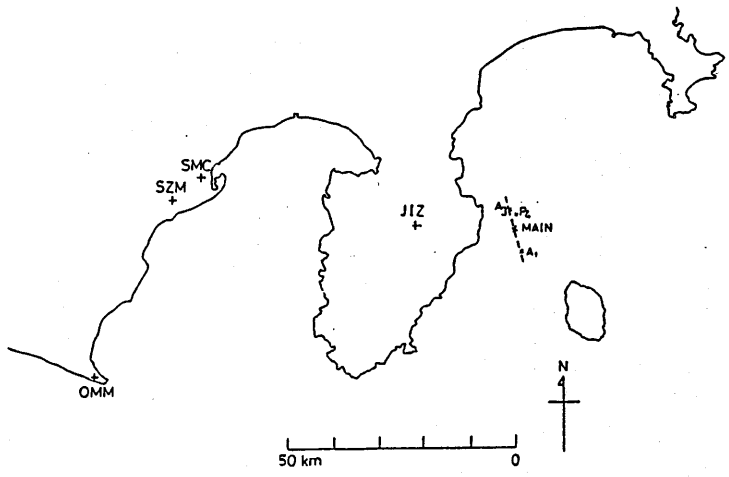

Fig. 2. The location of the observation sites and the epicenters of the mainshock and the small events used for synthesis.

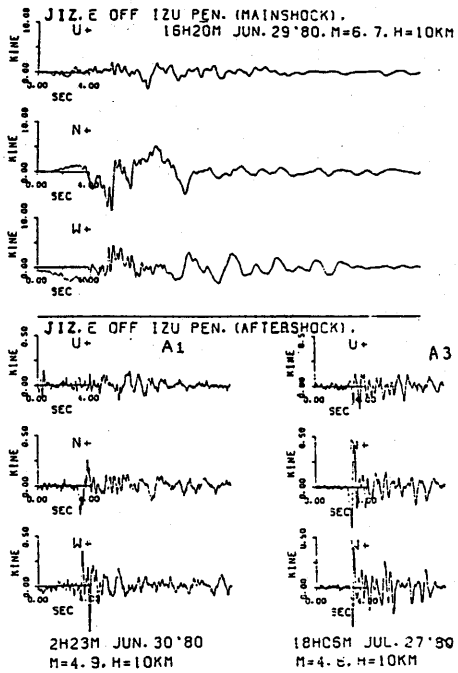

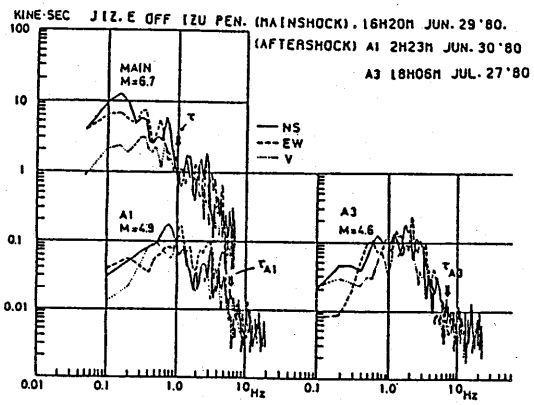

Fig. 4. The Fourier spectra of the mainshock and two aftershocks, A1 and A3.

Fig. 3. The observed seismograms of the mainshock and two aftershocks A1 and A3, at JIZ.

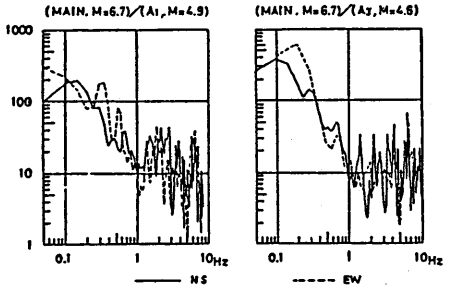

Fig. 5. The spectral ratio between the mainshock and aftershocks, A1 A3.

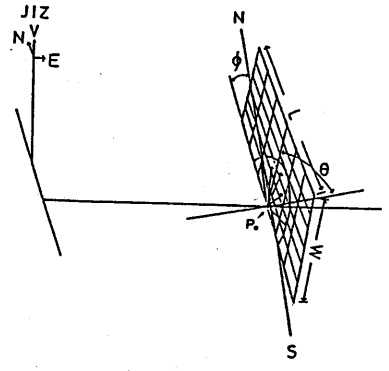

Fig. 6. The schematic model of the fault plane. Rupture spreads circularly from Po.

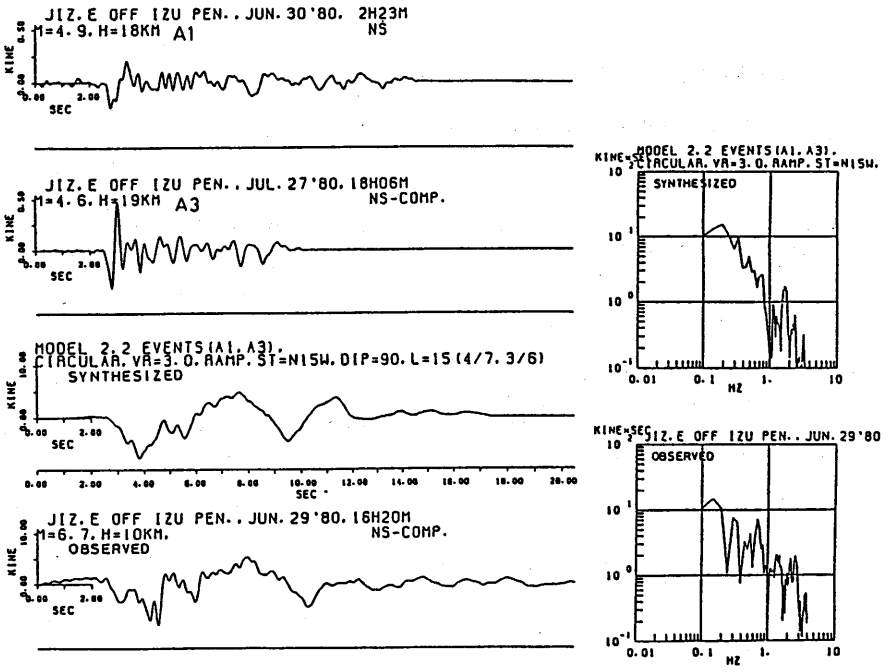

Fig. 7. Comparison of the synthesized velocity seismograms with the observed ones.

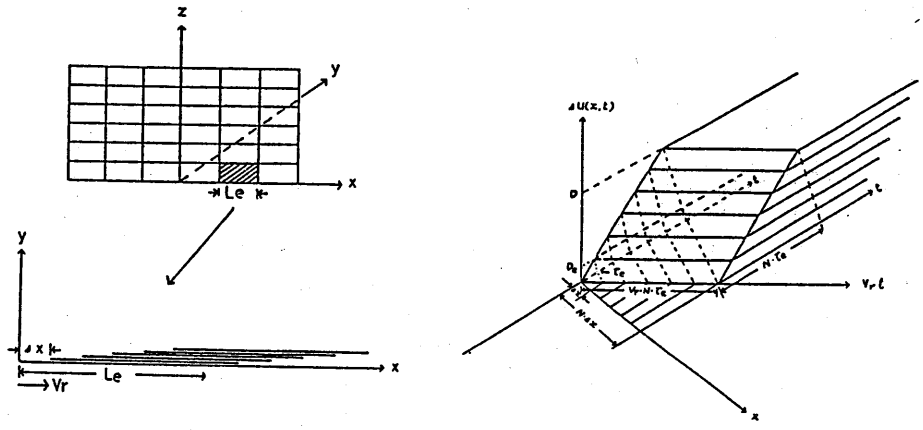

Fig. 8. (a) The distribution of subfaults during a large event. Each subfault corresponds to a small event. (b) The relation between the dislocation time function of the small event and that of the large event in time-space domain for the model shown in (a).

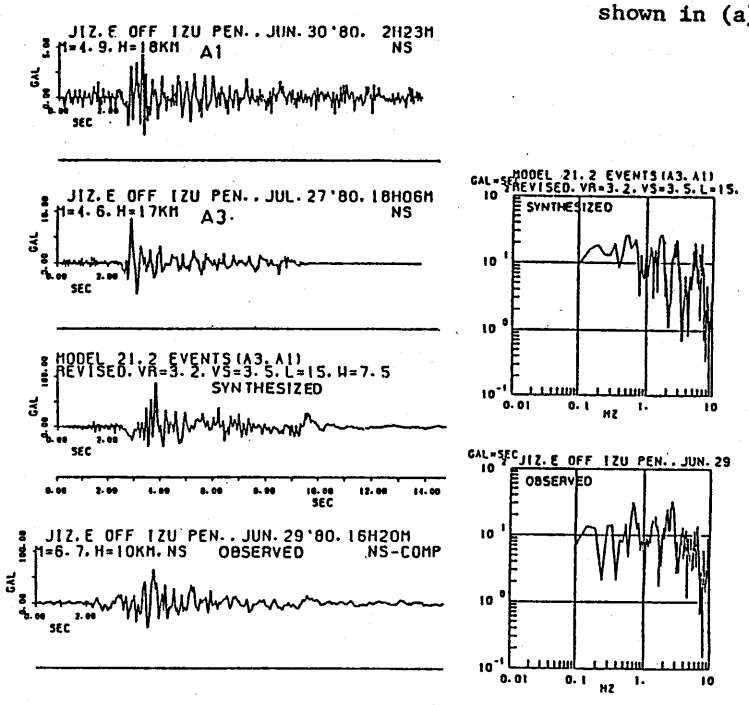

Fig. 9. Comparison of the synthesized acceleration seismogram by the revised method with the observed one.